

Power generation assessment of photovoltaic noise barriers across 52 major Chinese cities

Kai Zhang ^{a,c}, Dajiang Wang ^a, Min Chen ^{a,b,d,*}, Rui Zhu ^e, Fan Zhang ^f, Teng Zhong ^a, Zhen Qian ^a, Yazhou Wang ^a, Hengyue Li ^a, Yijie Wang ^a, Guonian Lü ^a, Jinyue Yan ^{c,g}

^a Key Laboratory of Virtual Geographic Environment (Ministry of Education of PRC), Nanjing Normal University, Nanjing 210023, PR China

^b International Research Center of Big Data for Sustainable Development Goals, Beijing 100094, PR China

^c School of Business, Society & Engineering, Mälardalen University, Västerås 72123, Sweden

^d Jiangsu Center for Collaborative Innovation in Geographical Information Resource Development and Application, Nanjing 210023, PR China

^e Institute of High Performance Computing (IHPC), Agency for Science, Technology and Research (A*STAR), Singapore 138632, Republic of Singapore

^f Institute of Remote Sensing and Geographical Information System, School of Earth and Space Sciences, Peking University, Beijing 100871, PR China

^g Department of Building Environment and Energy Engineering, The Hong Kong Polytechnic University, Hong Kong, PR China

HIGHLIGHTS

- A framework to assess the photovoltaic (PV) potential of noise barriers is developed.
- Building shadows are considered when assessing the PV potential of photovoltaic noise barriers (PVNB).
- The RNB mileage of each city is closely and positively related to the PV potential on RNBs.
- The annual power generation of PVNBs in China's 52 cities was estimated.

ARTICLE INFO

Original content: [Validation data \(Original data\)](#)

Keywords:

Road noise barriers
Photovoltaic
Building shadows
Sustainable cities

ABSTRACT

Photovoltaic noise barriers (PVNBs) have the potential to contribute to sustainable urban development by increasing the supply of renewable energy to cities while decreasing traffic noise pollution. However, estimating the power generation of PVNBs at the city or national scale remains a challenge due to the complexities of the urban environment and the difficulties associated with collecting data on road noise barriers (RNBs) and radiation. This study used RNBs, 2.5-dimensional (2.5D) buildings, and hourly time resolution radiation data, to estimate the power generation of PVNBs in 52 of China's major cities. First, hourly building shadows were estimated for each day of the year, covering the period from sunrise to sunset, to identify areas of RNB that are shaded at any given time. Second, hourly clear-sky radiation data were collected and corrected using a radiation correction model to simulate real weather radiation. Finally, utilizing an inclined surface radiation estimation model, the photovoltaic (PV) potential both inside and outside RNBs affected by building shadows was assessed. Subsequently, the power generation of PVNB was estimated based on parameters of mainstream PV systems in the market. The results show that the RNB mileage in 52 selected cities represents 87.7% of China's total RNB mileage. Building shadows often result in a radiation loss of approximately 30% for RNBs reception. The installed capacity and annual power generation of PVNBs in all investigated cities are 2.04 GW and 690.74 GWh, respectively. This study estimates the comprehensive PV potential of potentially exploitable PVNBs in China, offering essential scientific insights to inform and facilitate the strategic development of PVNB projects at both the national and municipal levels.

1. Introduction

In addition to being hubs of human activities and production, cities

are also densely areas in terms of buildings, transportation, political and economic activities [1]. Annually, cities consume 65% of the world's resources and energy, resulting in the generation of 75% of all greenhouse gases [2]. Therefore, achieving sustainable urban development

* Corresponding author at: School of Geography, Nanjing Normal University, No.1, Wenyuan Road, Qixia District, Nanjing 210023, PR China.
E-mail address: chenmin0902@163.com (M. Chen).

necessitates an increase in the proportion of renewable energy sources within cities and the enhancement of urban energy structures [3,4].

control of urban noise pollution. The spatial distribution of RNBs in China is characterized by larger cities in the southeast with higher levels

Nomenclature	
ω	Solar hour angle
ϕ	Latitude
δ	Solar declination angle
t_s	Solar time
n	The n -th day of the year
β	Slope angle of the RNB
φ	Azimuth angle of the solar
θ_z	Zenith angle of the solar
h	Altitude angle of the solar
γ	Azimuth angle of the RNB
$GI_{\beta\gamma}$	Global irradiance received by RNB, W/m^2
$DI_{\beta\gamma}$	Diffuse irradiance received by RNB, W/m^2
$DBI_{\beta\gamma}$	Direct beam irradiance received by RNB
$RGI_{\beta\gamma}$	Ground reflected irradiance received by the RNB, W/m^2
R_b	Beam irradiance conversion ratio
$K_{b,f}$	Anisotropy indexes of the diffuse irradiance
I_0	Extraterrestrial irradiance on a horizontal surface
N	Number of solar panels in each city
M_{dif}	Monthly average diffusion ratio
P_{clear}	Percentage of monthly clear weather
$P_{partlycloudy}$	Percentage of monthly partly cloudy weather
P_{cloudy}	Percentage of monthly cloudy weather
$GI_{\beta\gamma}^i$	The i -th PVNB that received total solar irradiance in a year, W/m^2
i	The i -th RNB
n_1	Number of RNBs in each city
d	The d -th day of the month
n_2	Actual number of days in each month
M_{trans}	Monthly average atmospheric transmittance
t	The time in a 24-h system
S_i	Area of the i -th PVNB, m^2
E_P	Power generation of PVNB, kWh
P_{AZ}	Installed capacity of the PVNBs, GW
H	Average peak sunlight hours of the PV system
K	Overall performance coefficient of the PV system
E_s	Standard test condition for photovoltaics equalling 1000 W/m^2
P	Rated power of a single solar panel, W

Photovoltaic (PV) is an important renewable energy supply in the IEA's Net Zero Emissions by 2050 Scenario [5]. Globally, the total installed PV capacity reached 945.8 GW by the end of 2021 [6]. Driven by goals to achieve carbon peak and neutrality, China had also achieved an installed PV capacity of 305 GW by the end of 2021 [7]. PV power generation has now reached a level where it can effectively compete with traditional fossil fuel-based power generation [8]. However, regional variations in solar resources and land-use restrictions have resulted in significant geographical imbalances in China's PV capacity distribution [9]. The disparity between the supply and demand for electricity and the high cost of long-distance power transmission has contributed to the high abandonment rate of PV generation in Northwest China [10]. Consequently, the development of distributed PV systems, which do not require long-distance power transmission, could efficiently boost the supply of renewable energy in urban areas with high energy demands. Currently, distributed PV solutions, such as rooftops and building façade PV [11,12], highway PV [13], high-speed railway PV [14], photovoltaic noise barrier (PVNB) [15], and other infrastructure that can be integrated with PV systems [16], have been investigated in many cities.

In urban environment, the restricted areas of building rooftops, the difficulty of identifying property rights, and the safety issues associated with PV panel installation present several practical obstacles for rooftop PV construction [17]. Alternatively, road noise barriers (RNBs) can provide abundant space to deploy PV systems to generate clean energy and provide complementary power generation. As early as 1989, PVNBs were proposed and applied in practical engineering in certain European nations [18]. However, because of the high cost of PV modules and low PV conversion efficiency, PVNBs have not been popularized. In recent years, due to the development of PV technology and the rise in PV efficiency, there has been a growth in interest in PVNBs [19,20].

PV panels can be integrated with RNBs and used as distributed PV systems without the need for additional land. Therefore, PVNB can be utilized in crowded metropolitan areas without additional land purchase expenditures. Additionally, PVNBs deployed along roads are generally easy to construct and maintain [21]. The economic and social benefits of PVNBs may also help accelerate the building of RNBs and promote the

of urbanization having longer RNB mileages [22]. In China's northwest, there are numerous huge and super-large scale PV facilities because of the excellent irradiance conditions and greater and more concentrated undeveloped land resources [23]. But nevertheless, due to the lower population and smaller city sizes, power demand is significantly lower in the northwest than in the southeast of China [24]. In contrast, the southeast, with its strong energy demand, faces limitations in constructing PV facilities due to irradiance conditions and land resources, despite the high energy demand. Therefore, the installation of PVNBs in southeastern cities has the potential to mitigate the regional mismatch between PV generation and energy demand to some extent. Furthermore, as sustainable urban development continues, it is expected that more RNBs will be constructed and improved [25]. This will lead to an increasing number of RNBs available for the installation of PV systems in urban environments. Consequently, the application potential of PVNBs is on the rise.

Estimating the potential of PVNBs on city scales is a challenging task. Access to information regarding the mileage and geographical distribution of RNBs is not readily available to the public, data on radiation with high spatial and temporal resolutions are scarce. Additionally, RNBs are often constructed in proximity to buildings, and the shadows cast by these structures reduce the amount of solar radiation that PVNBs can receive. Current research on PVNB potential has focused on two aspects: 1) At the microscopic scale, the performance of PV panels installed on RNBs with different orientations and angles was tested under real weather conditions [26,27]. Some experiments have also been used to investigate the performance comparison of single-sided and double-sided PVNB, and the quantification of the shading effects from opposing sides in double-sided PVNBs, have also been conducted [28]. Researchers also exploring the optimized PVNB design patterns that achieves a balance between economic viability, energy output, and noise control [29]; 2) At the city or national scale, related researchers have gathered RNB information from street-view images and applied deep learning methods to assess the energy potential of PVNBs [30]. Other studies have evaluated the PVNB potential through field investigations of the distribution of RNBs [19,31]. However, national scale estimates of PVNB potential are inferred from the results of accurate predictions in a

small range of locations [32]. Additionally, radiation estimates rely on specialized software and are primarily based on low-resolution observation site data, posing potential limitations. Therefore, the studies mentioned above have not consistently yielded reliable results in estimating PV potential in large areas.

Based on the above analysis, it is evident that there are limited references exploring a framework for precisely estimating the PV potential of PVNBs at city scales. Additionally, almost none of the afore mentioned studies considered the impact of building dynamic shadows in urban environments on the PV potential of PVNBs. Therefore, this study proposes a framework for the precise assessment of the PV potential of PVNBs at city scales, considering the impact of building shadows. This study makes the following contributions:

- 1) Proposed a refined framework for the accurate assessment of the PV potential of PVNBs at city scales, utilizing precise attributes information of RNBs, high-time-resolution radiation data, and an optimized radiation estimation model.
- 2) Dynamic shadows cast by buildings on RNBs were considered for the first time when estimating the PV potential of PVNBs at city scales, and the resulting loss in PV potential caused by building shadows has been quantified.
- 3) Identified the features of the regional distribution of the PVNBs potential and estimated the PV potential and power generation of PVNBs in China, providing guidance for planning PVNBs in each region in accordance with local conditions.

The remainder of the paper is organized as follows. Section 2

introduces the study area and related data. Section 3 systematically illustrates the methods employed for building shadow simulation and the estimation of PV potential. Section 4 offers a comprehensive analysis of the characteristics of building shadows and the results of PV potential estimation for PVNBs. Sections 5 and 6 present the conclusion and discussion of this study, respectively.

2. Study area and materials

2.1. Study area

China now has 363 prefecture-level cities [33]. However, only 226 prefecture-level cities have RNBs, and in most of them, the RNB mileage is less than 5 km [22]. Because of the huge cost of estimating PV potential of PVNBs, only cities with RNB mileages greater than 5 km are considered. Deyang, Datong, and Zunyi were not included in the study area even though their RNB mileages are longer than 5 km because 2.5-dimensional (2.5D) building data could not be obtained. Fig. 1 depicts the 52 prefecture-level cities with RNB mileages greater than 5 km (the province of Taiwan was not included in this study due to the lack of RNB data).

2.2. Data sources

Vectorized RNBs were provided by the National Tibetan Plateau Data Center (<http://data.tpdc.ac.cn>). Machine learning was used to identify RNBs in China from Baidu Street View images, and ArcGIS Pro was used to vectorize the result [22]. In 363 prefecture-level cities in China, the

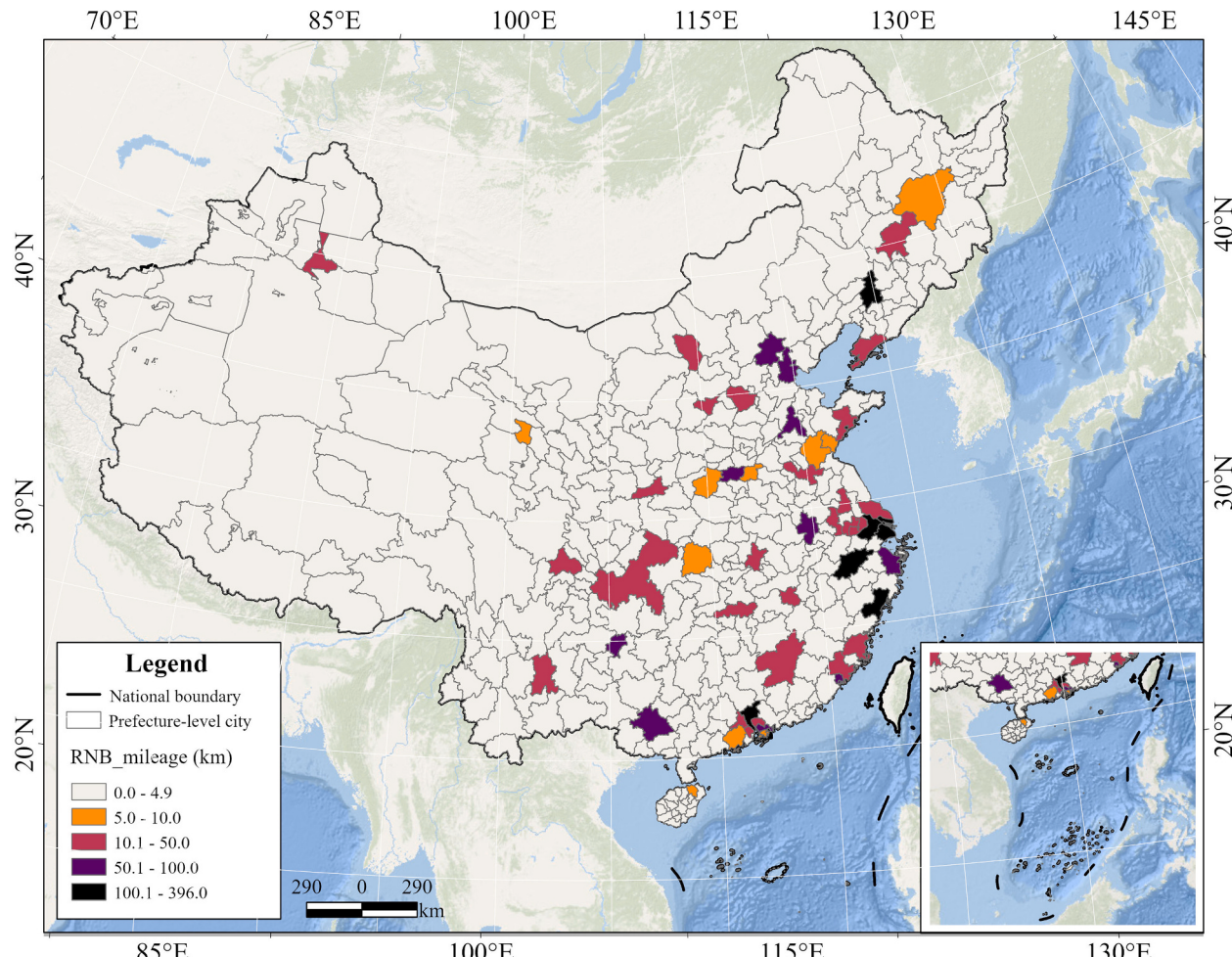


Fig. 1. Spatial distribution characteristics of RNBs in China.

vectorized RNB data were applied to calculate the total mileage of existing RNBs and obtain the spatiotemporal distribution of completed RNBs. 2.5-D buildings were considered, and data were collected from Baidu Maps. In building shadow calculations, the height attribute of each building is utilized to stretch each vertex of the building, resulting in the formation of a regular polyhedron. Corresponding radiation data were collected from the Copernicus Atmosphere Monitoring Service (CAMS) (<https://www.soda-pro.com/web-services/radiation/cams-radiation-service>), which provides time series of global, direct, and diffuse irradiation on horizontal surfaces and direct irradiation on the normal plane under the clear-sky conditions. The irradiation statistics for a city are obtained directly from CAMS based on the latitude and longitude of the city. World Weather Online (<https://www.worldweatheronline.com>) provides daily statistical data for meteorological parameters in the corresponding cities. The number of sunny and cloudy days per month, for example, in this study, can be used to calibrate the data for clear-sky irradiation. After correction, the clear-sky radiation data are closer to the radiation values under actual weather circumstances, thus improving the accuracy of the corresponding estimation results.

3. Methodology

In this study, the PVNB potential is calculated as follows: first, the RNB areas that shadowed by building at corresponding times are determined by calculating the hourly building shadows in each city using Baidu building data and Pybdshadow [34]; then, to estimate the radiation under actual meteorological conditions, the clear-sky radiation for each city is corrected using meteorological parameters; finally, the PV potential of PVNBs is estimated with reference to the inclined surface radiation assessment model and current mainstream PV system parameters. Fig. 2 illustrates the technical flow chart used in this approach.

3.1. PVNB shading analysis based on building shadows

Building shadows in urban environments may have a greater impact the amount of solar energy that PVNBs receive. Therefore, when calculating the PV potential on RNBs, the areas shaded by building shadows need be identified. Since the sun's position changes throughout

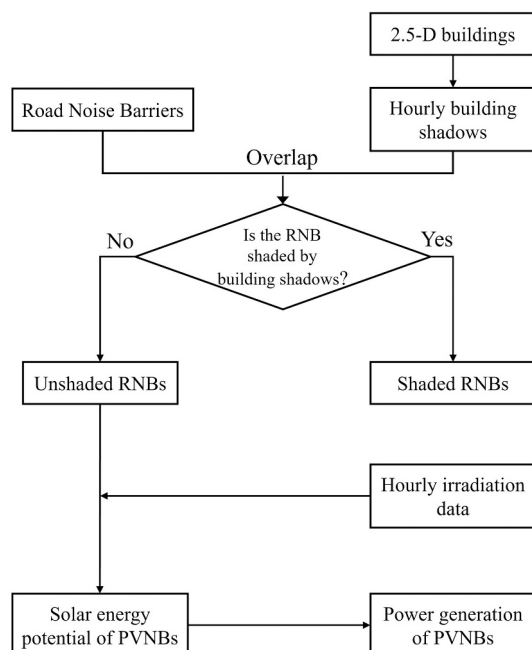


Fig. 2. Flowchart for estimation PV potential of PVNB.

the day, building shadows also change accordingly. Performing real-time building shadow calculations, however, is time-consuming and requires extensive computational resources. Therefore, in this study, the hourly variation characteristics of building shadows are calculated to consider the accuracy and efficiency of building shadow calculations. Additionally, at the monthly scale, the variations in parameters such as the solar altitude angle and azimuth angle in each city are comparatively small. Therefore, the day in the middle of each month is selected to calculate the building shadow areas, and this result is used to represent the building shadow area on each day of that month.

The hourly areas of building shadows in each city are calculated using a Python extension package known as Pybdshadow. Pybdshadow can generate building shadows over large areas based on sunlight. It uses the provided location and time data to utilize sun position information and building height attributes, ultimately creating shadow geometry data.

In Fig. 3, The rectangle represents the building, h is the height of the building, the red rays represent the sun rays, α , and γ is the solar altitude and azimuth angle at a particular moment in time at a certain place, which can be calculated from the given latitude and time [13]. Pybdshadow can compute the shadows cast on the ground by the individual face vertices of a 2.5D building model after it has been illuminated by the sun. then, by connecting the ground-level vertices of each face, the shadow area of the building at that specific instant can be determined. In Fig. 3, the gray shaded area represents the shadow cast by the building. The blue line L represents the RNB, and the line mn indicates the portion of the RNB that is obscured by the building shadow. It is important to note that the height of the RNB is not regarded when determining whether it is obscured. Only a 2-dimensional perspective is employed to determine if the RNB overlaps the building shadows on the ground.

The sunrise and sunset times differ from city to city due to spatial and time zone differences. Therefore, each city's sunrise and sunset time are calculated separately, and then the areas of building shadows are determined for each hour from sunrise to sunset. The sunrise and sunset time for each city are calculated with the following formulas:

$$\cos\omega = - \tan\phi \times \tan\delta \quad (1)$$

$$\omega = 15^\circ (t_s - 12) \quad (2)$$

where ω is the solar hour angle, ϕ is the latitude of each city, δ is solar declination, and t_s is the solar time [35].

The solar hour angle provides a measure of the angular separation between the sun at solar noon and the sun at a local solar time. The latitude of each city can be acquired from a geographic shapefile. Solar declination is the angle between the incoming solar rays and the plane of the Earth's equator. Eq. 3 shows the formula for calculating solar declination.

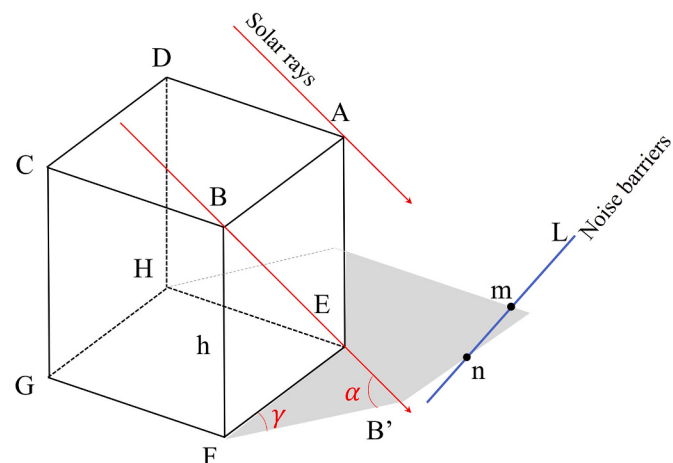


Fig. 3. Schematic diagram of building shadow calculation principle.

$$\delta = 23.45^\circ \times \sin\{360^\circ \times [(284 + n)/365]\} \quad (3)$$

where δ is solar declination, n is the n -th day of the year, and 23.45° is the tilt angle of the Earth. Based on the above formulations, the sunrise and sunset times on representative days were acquired.

However, only buildings that are within a certain distance from RNBs have the potential to obstruct the solar radiation that RNBs receive. Not all buildings in cities impede the solar radiation that RNBs receive. Additionally, calculating the shadows cast by each building in each city at a given time would require considerable time and computational resources. Therefore, it was assumed that all buildings in each city theoretically had no influence on the solar radiation received by the RNBs at any time of the year if they did not shadow the surrounding RNBs when their shaded areas were at a maximum. The shadow areas of buildings in most Chinese regions are greatest during the winter solstice, when the sun is directly above the Tropic of Capricorn. Therefore, on the day of the winter solstice, the hourly shadow areas from sunrise to sunset of all buildings in each of the 52 cities were calculated. The shadows cast by certain buildings in the cities at the time of sunrise or sunset on the winter solstice do not have any influence on the solar radiation received by RNBs. These buildings were excluded from the calculation of the annual building shadow areas to improve the efficiency of the RNB shadow analysis. Additionally, the calculation of building shadows close to the time of sunrise or sunset will produce an infinite area of building shadows, which will cause the model to take a long time to produce shadow files. This is because the sun is near the horizon at this time, the solar altitude angle is close to 0, and the solar radiation is also close to 0. Therefore, all building shadows were calculated beginning one hour after sunrise and one hour before sunset.

3.2. Solar energy potential estimation for RNBs

To make the estimation approach more feasible, only those parameters in this study that significantly affect the PV potential of PVNB are considered. These factors are the latitude, area, slope, and azimuth of the RNBs. Assuming that all RNBs in China are vertical and 3 m tall, the

slope of the RNB is 90° . The RNBs in all cities were segmented at 20 m intervals to obtain the azimuth of each RNB segment. Then, the area of each segment of each RNB is acquired. The azimuth and altitude of an RNB can be directly acquired from vectorized RNB data. Additionally, the PV panels are assumed to be installed on the top of RNBs, leaving little space at the bottom to avoid shading from surrounding weeds or low vegetation [32]. Some space also needs to be reserved for maintenance and the servicing of the RNBs and PV modules. Therefore, it is assumed that 70% of the area on the top of RNBs is available for PV panel installation, and PV panels are mounted vertically on both sides of the RNBs. Next, using solar radiation conversion models for horizontal and inclined surfaces, the solar radiation received by a vertically installed PVNB can be calculated based on the available surface radiation data [36]. Fig. 4 illustrates the detailed procedure used to calculate the solar potential of PVNBs.

Fig. 5 depicts the relationship between RNB and incident sunlight. The solar radiation that reaches an inclined ground surface is composed of three types of irradiances: direct beam irradiance, diffuse irradiance, and ground reflected irradiance. Eq. 4 is applied to calculate the global irradiance that RNB received [37]:

$$GI_{\beta\gamma} = DBI_{\beta\gamma} + DI_{\beta\gamma} + RGI_{\beta\gamma} \quad (4)$$

where β is the slope angle of the RNB, γ is the azimuth angle of the RNB, $GI_{\beta\gamma}$, $DBI_{\beta\gamma}$, $DI_{\beta\gamma}$, and $RGI_{\beta\gamma}$ are the global irradiance, direct beam irradiance, diffuse irradiance, and ground reflected irradiance received by the RNB, respectively. Eq. 5 is applied to calculate $DBI_{\beta\gamma}$ in Eq. 5 [38,39]:

$$DBI_{\beta\gamma} = BHI \times R_b \quad (5)$$

where BHI is beam irradiation on horizontal plane and R_b is the beam irradiance conversion factor, that is, the ratio of the direct beam irradiance on a tilted surface to that on the horizontal surface.

$$R_b = \max\{[\cos\beta \times \sinh + \sin\beta \times \cosh \times \cos(\varphi - \gamma)] / \cos\theta_z, 0\} \quad (6)$$

where β is the slope angle of the RNB, φ is the azimuth of the solar, γ is

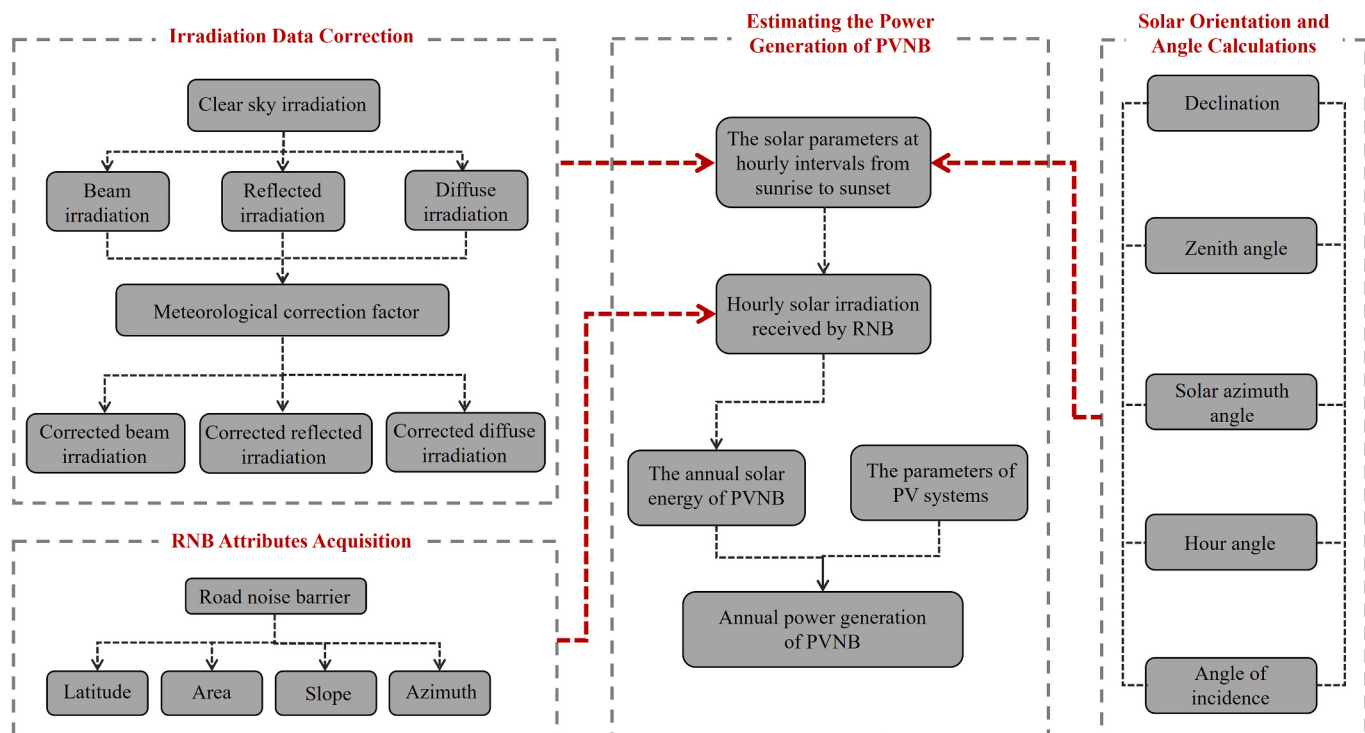


Fig. 4. Detailed technical procedures for estimating PVNBs power generation.

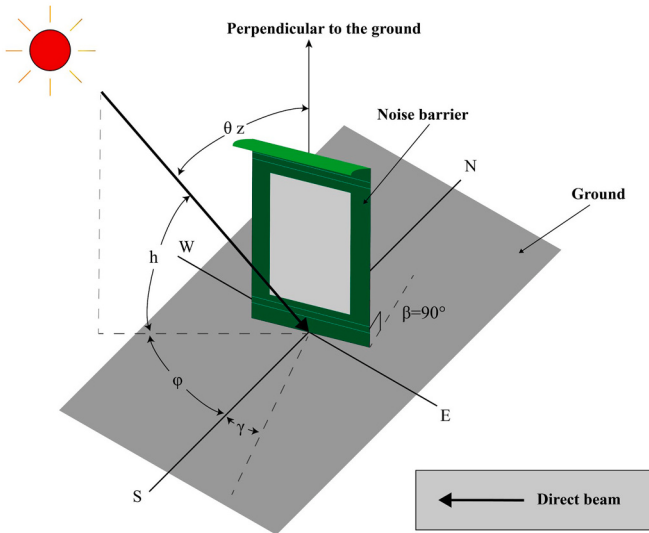


Fig. 5. Schematic diagram of the relationship between incident sunlight and RNB, where β is the slope angle of the RNB. γ , θ_Z , and h is the azimuth angle, zenith angle, and altitude angle of the solar, respectively [30].

the azimuth angle of the RNB, and θ_Z is the solar zenith angle ($\theta_Z = 90^\circ - h$). According to Eqs. 5 and 6, $DBI_{\beta\gamma}$ can be acquired.

$DI_{\beta\gamma}$ cannot be obtained directly, it needs to be calculated based on the horizontal diffuse irradiance as follows [36]:

$$DI_{\beta\gamma} = DHI \times \left\{ (1 - K_b) \times (1 + \cos\beta) / 2 \times \left[1 + f \times \sin^3\left(\frac{\beta}{2}\right) + K_b \times R_b \right] \right\} \quad (7)$$

where K_b and f are the anisotropy indexes of the diffuse irradiance and DHI is the diffuse irradiance on a horizontal surface.

The formulas for the anisotropy indexes are as follows:

$$K_b = \min\left[\frac{(GHI - DHI)}{I_0}, 1\right] \quad (8)$$

$$f = (DNI/GHI)^{0.5} \quad (9)$$

where GHI is the global irradiance on a horizontal surface, DNI is the direct normal irradiance, and I_0 is the extraterrestrial irradiance on a horizontal surface.

Due to the expensive cost of data collection and significant environmental variations across different regions, it is difficult to obtain ground reflected irradiance for large-scale areas. Therefore, this study reference related study to assessment the $RGI_{\beta\gamma}$ [40]:

$$RGI_{\beta\gamma} = GHI \times \rho \times (1 - \cos\beta) / 2 \quad (10)$$

where ρ is the ground reflectivity (or albedo), typically assumed to be 0.2 for most ground surfaces, is a mean value proposed by Liu & Jordan [41] that is widely accepted and used in applications where albedo measurements are not available.

The influence of clouds on solar radiation under actual weather conditions must be considered, as the radiation data acquired in this study are radiation values under clear-sky conditions. The monthly average atmospheric transmittance and diffuse emissivity are calculated using monthly statistics for clear, partly cloudy, and cloudy days with reference to related studies. Then, the clear-sky radiation data are corrected. The daily sunshine hour statistics for 52 cities were obtained from World Weather Online. In this study, clear days are defined as days with more than 8 h of sunshine, cloudy days are defined as days with less than 3 h of sunshine, and those days with between 3 and 8 h of sunshine are defined as partially cloudy days with reference to the relevant

radiation correction model [42]. Eqs. 11 and 12 are the equations for the monthly average atmospheric transmittance and monthly average diffuse ratio, respectively [43].

$$M_{trans} = 0.70 \times P_{clear} + 0.50 \times P_{partlycloudy} + 0.30 \times P_{cloudy} \quad (11)$$

$$M_{dif} = 0.20 \times P_{clear} + 0.45 \times P_{partlycloudy} + 0.70 \times P_{cloudy} \quad (12)$$

where M_{trans} is the monthly average atmospheric transmittance, M_{dif} is the monthly average diffusion ratio, P_{clear} is the percentage of monthly clear weather, $P_{partlycloudy}$ is the percentage of monthly partly cloudy weather, and P_{cloudy} is the percentage of monthly cloudy weather.

when assessing the $RGI_{\beta\gamma}$ under the actual weather conditions, this study referenced the related study to correct the clear-sky GHI by monthly average atmospheric transmittance [44]. Therefore, the total solar radiation received by an RNB under actual weather conditions is $GI_{\beta\gamma}^i$:

$$\begin{aligned} GI_{\beta\gamma}^i = & \sum_{m=1}^{12} \left(\sum_{d=1}^{n_2} \left(\sum_{t=0}^{23} DBI_{\beta\gamma} \times M_{trans} \right) \right) \\ & + \sum_{m=1}^{12} \left(\sum_{d=1}^{n_2} \left(\sum_{t=0}^{23} DI_{\beta\gamma} \times M_{dif} \right) \right) \\ & + \sum_{m=1}^{12} \left(\sum_{d=1}^{n_2} \left(\sum_{t=0}^{23} RGI_{\beta\gamma} \times M_{trans} \right) \right) \end{aligned} \quad (13)$$

where $GI_{\beta\gamma}^i$ is the i -th RNB that received total solar radiation in a year, i is the i -th RNB ($i = 1, 2, 3, \dots, n_1$), and m represents the month ($m = 1, 2, 3, \dots, 12$). Here, d is the d -th day of the month, n_2 is the actual number of days in each month, and t is the time in a 24-h system ($t = 0, 2, 3, \dots, 23$).

The following formula is applied to estimate the total solar radiation (TSR) of all RNBs in all cities in each full year:

$$TSR = \sum_{i=1}^{n_1} (S_i \times GI_{\beta\gamma}^i) \quad (14)$$

where S_i is the area of the i -th PVNB, i is the number of RNBs ($i = 1, 2, 3, \dots, n_1$), where n_1 is the total number of RNBs in each city, and TSR is the total solar PV potential of the target RNB system for one year.

3.3. Electricity generation estimate for PVNBs

The rated power, installed capacity, and PV conversion efficiency of a PV system must all be determined to estimate its electricity production. Two mono-facial PV panels with dimensions of $1 \text{ m} \times 1 \text{ m}$ and a rated power of 200 W were installed on the outside and inside of RNBs. This information was obtained by referring to an existing study [45]. Then, the total electricity generation of each PVNB system in each city was calculated using the following equation:

$$E_P = P_{AZ} \times H \times K \quad (15)$$

where E_P is the generation of solar-PV electricity, P_{AZ} is the installed capacity of the target solar-PV system, H is the average peak sunlight hours of the PV system, and K is the overall performance coefficient of the solar-PV system, with a general value of 0.8 [46]. The average peak sunlight hours can be calculated with the following equation.

$$H = \frac{TSR}{S \times E_s} \quad (16)$$

where TSR is the total solar radiation potential of all RNBs in each city, S is the area of solar panels installed on the RNBs, and E_s is the standard test condition for PV equalling 1000 W/m^2 . The installed capacity of a solar PV system is calculated based on the rated power P of a single solar panel and the number N of solar panels in the solar PV system using the following equation:

$$P_{AZ} = P \times N \quad (17)$$

where P is the rated power of a single solar panel and N is the number of solar panels in each city.

4. Result

4.1. Spatio-temporal characteristics of the effect of building shadows on RNBs

Hourly building shadows were calculated for each city from sunrise to sunset in 2021 using the method described in Section 3.1. The areas of RNBs shaded at a corresponding time were determined by overlaying the RNB data with the hourly building shadows. Fig. 6 illustrates the hourly building shadows of parts of Guangzhou's buildings on December 15, 2021, as well as the spatial relationship between RNBs and building shadows. As depicted in Fig. 6, various regions of RNBs experienced shading by buildings at 8 a.m., 10 a.m., and 4 p.m. This study provides an in-depth investigation into the character and extent of the influence that building shadows have on RNB, nine representative cities were selected for this study based on the geographic distribution and RNB mileage characteristics of 52 cities. For each of the nine selected cities, the hourly RNB area shaded by buildings was calculated using the dates of June 15 and December 15, 2021. Further calculations were made to calculate the proportion of the RNB shaded by buildings to the overall RNB area. Fig. 7 shows the temporal change characteristics of the RNB area shaded by building shadows at the corresponding dates for the nine representative cities.

The red curve in Fig. 7 depicts how, in each representative city, the ratio of the RNB shaded by building shadows varied from sunrise to sunset on December 15. As above, the black curve shows how each city changed on June 15. The blue area between the black and red curves represents the interannual variation range in the RNB area shaded by building shadows. The purple and green curves show the intensity of solar radiation in each city on December 15 and June 15, respectively. The RNB in each city is minimally shaded by building shadows in June and maximally shaded in December, as shown in Fig. 7, at the same time

of the year. In addition, the proportion of RNBs obscured by building shadows varies considerably less over the year in low-latitude cities (e.g., Hangzhou and Guangzhou) than in high-latitude cities (e.g., Harbin and Urumqi), which is represented by the blue area in Fig. 7. Notably, between 9 a.m. and 3 p.m. in June, less than 10% of the RNB area in most of these cities was shaded by building shadows. In certain cities, an RNB area is even less than 10% of the time shaded by building shadows from 8 a.m. to 16 p.m. Between 9 a.m. and 15 p.m. in December, Shanghai, Hangzhou, Guangzhou, and Beijing, the shaded areas were also less than 30%. The remainder of the cities, except for Urumqi and Harbin in the high latitudes, had RNB shadow coverage rates of less than 35% and 40% over the same period in December. However, the intensity of solar radiation is relatively low during the one to two hours after sunrise and before sunset (Fig. 7). Therefore, despite being obscured by building shadows during these periods, the RNB lost only a small amount of solar energy.

4.2. Spatio-temporal characteristics of PVNB solar energy

Acquired the hourly shadowed areas of RNB caused by building shadows, the hourly solar energy potential of unshaded areas of RNB can be calculated according to the method described in Section 3.1. As this study assumes that 70% of the RNB area is available for installing PV panels, the hourly solar energy of the PVNB is calculated using 70% of the RNB area without shading from buildings as model input. The yearly solar potential of the PVNB can then be calculated by accumulating the hourly solar potential of the available RNB area. According to the findings in this study, the total solar potential of PVNB for 52 cities amounts to 4,317 GWh in 2021. Fig. 8 displays the distribution of the annual PVNB solar energy potential for these 52 cities.

Fig. 8 shows that most cities with high PVNB potential are in the eastern coastal cities of China. This is because the eastern coastal cities have greater urbanization and a more developed economy, both of which contribute to the construction and development of RNB. It is also likely that the demand for RNB construction is stronger in these cities since they are larger and have a higher density of urban roadways. This result demonstrates that the RNB mileage is the primary factor affecting

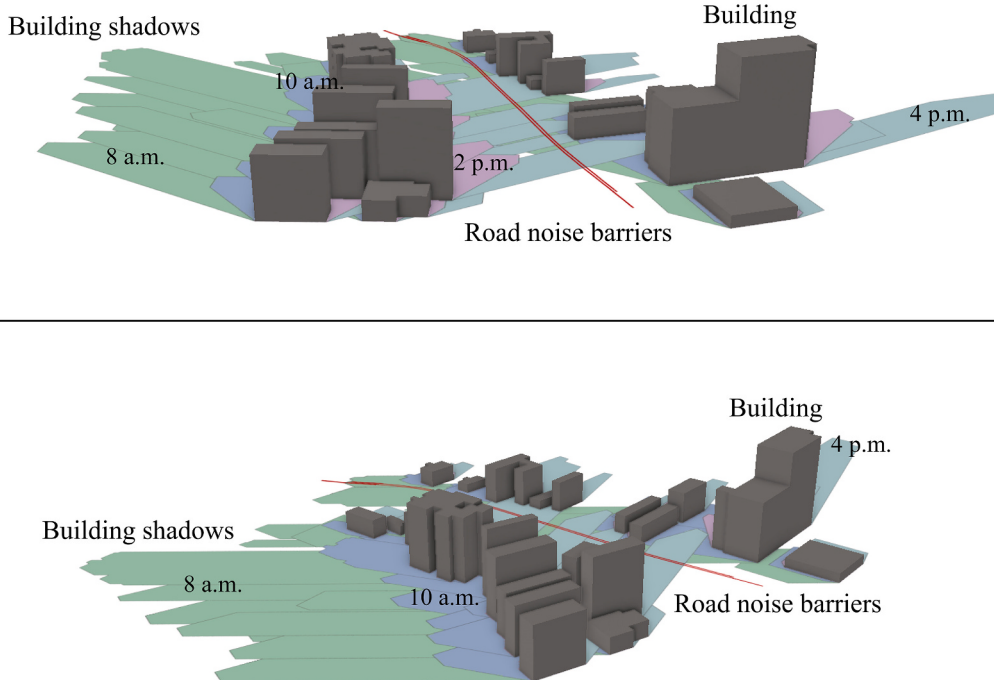


Fig. 6. The spatial positional relationship of 2.5D buildings, hourly building shadows, and road noise barriers in Guangzhou was examined from two perspectives on December 15, 2021.

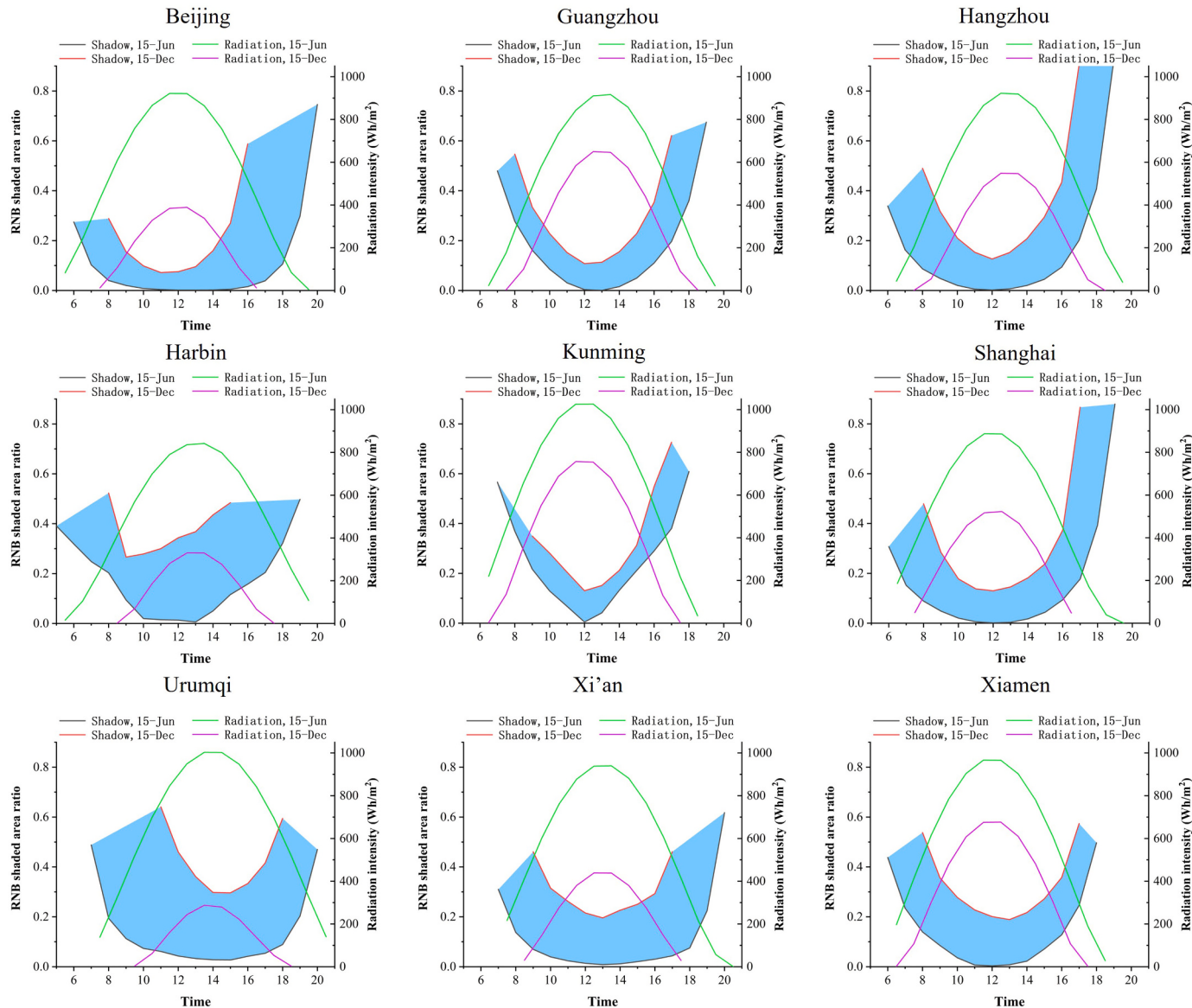


Fig. 7. Characteristics of the PVNB area shaded by building shadows in representative cities. The left axis represents the area ratio of RNB shaded by building shadows, the right axis represents the irradiance intensity of each city.

the amount of solar energy potential received by the PVNB in each city. Among the 52 cities, Shanghai, Suzhou, Guangzhou, Wuhan, Shenyang, and Beijing are the top six cities with the largest solar energy potential of PVNB. Correspondingly, these major cities are typically net energy-consuming regions since they are often regions with a high concentration of energy-intensive activities, such as human production and living, transportation, and manufacturing. In contrast, the potential for PVNB solar energy in midwestern cities is lower because of their smaller urban scale and shorter RNB distance. Therefore, this geographical distribution characteristic of the solar energy potential of PVNBs will also help to alleviate the regional imbalance between installed PV capacity and electricity demand in China.

To quantify the impact of building shadows on the solar energy received by RNBs and to describe the temporal variation of hourly solar energy received by RNBs, this study also analyses the hourly solar energy, annual solar energy both shadowed and unshadowed by buildings, and the annual solar energy received both inside and outside RNBs for nine selected representative cities. Fig. 9 illustrated the statistics results. In Fig. 9, the blue, purple, and black dashed lines represent the city's estimated solar energy without and with building shadows on the RNB's

solar radiation and solar radiation loss rate as a result of building shadowing. In selected nine representative cities, the loss rate between about 20% and 30%. The RNBs in Xi'an were least affected by building shadows, and the radiation loss rate was 20.71%, which may be related to the city's building height restriction policy. The impact of building shadows on the reception of RNB radiation in the remaining eight cities is generally around 30%. This suggests that the influence of building shadows on PVNB solar potential is quite significant in complex urban environments.

In Fig. 9, the red, green, and orange lines represent the cities' hourly solar energy received by outside, inside, and bifacial RNBs on July 15th, 2021, respectively. When observing the solar energy received by the inside and outside sides of RNBs, it was noticed that the solar energy received by the inside and outside sides of noise barriers in Beijing, Guangzhou, Hangzhou, and Shanghai is essentially identical. It also demonstrates that the quantity of solar energy received by the inside of the RNBs is marginally greater than that received by the outside. Before 10 a.m., Harbin receives more solar energy on the outside of the RNB than on the inside. After 10 a.m., the reverse pattern is observed, which may be due to the long east-west RNB mileage of the city. In Urumqi and

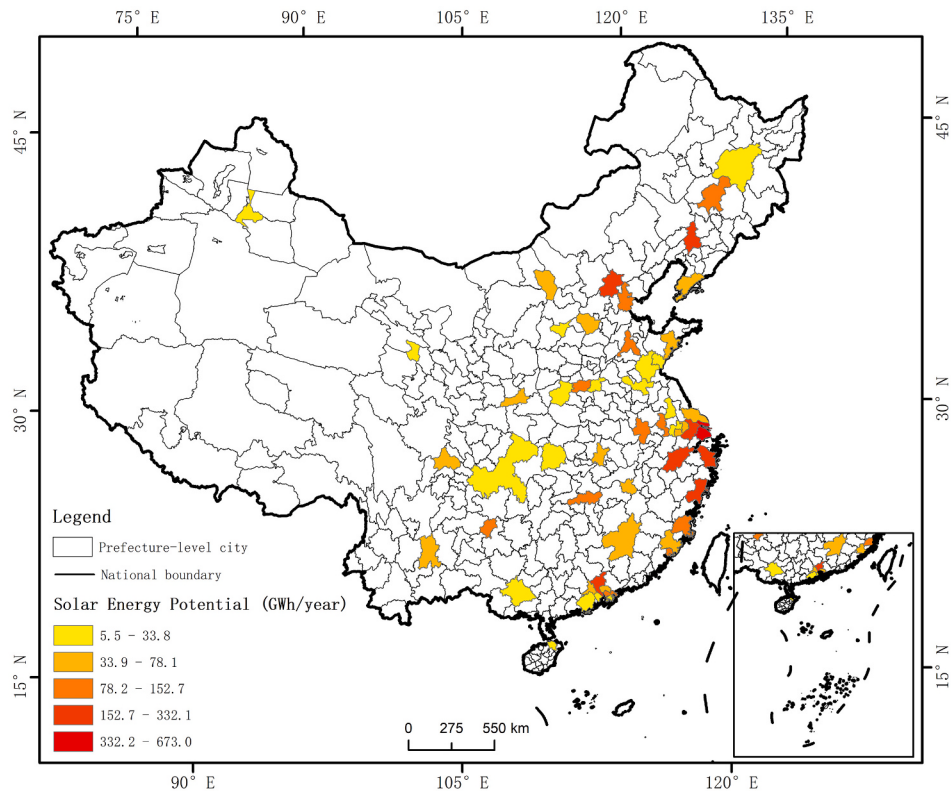


Fig. 8. Spatial distribution of the PVNB solar energy potential in 2021 for the 52 cities.

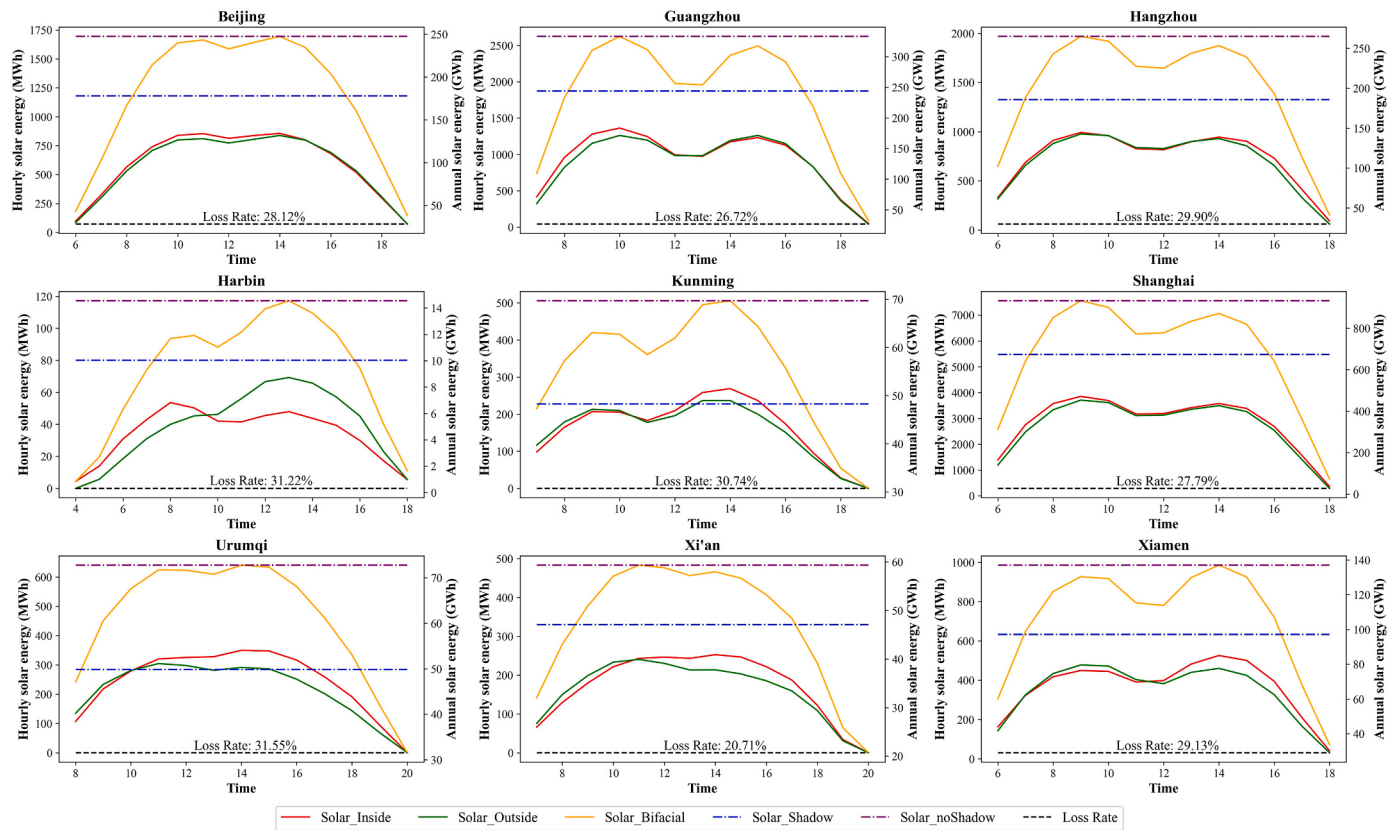


Fig. 9. Building shadows impact, hourly, and annual solar energy characters of RNBs.

Xi'an, before 10 a.m. or 11 a.m., it receives more solar energy on the inside of the RNB than on the outside. After 10 a.m. or 11 a.m. also illustrated a reverse pattern, indicating that the north-south mileage of RNBs is greater than that of RNBs with other orientations. Examining the orange line reveals that in cities with higher latitudes, the RNB receives more solar irradiation at noon, and the trough is less pronounced. This phenomenon is evident in cities like Beijing, Xi'an, and Urumqi. Conversely, in lower latitude cities where solar altitudes approach 90°, vertically positioned RNBs receive less solar energy.

In addition, this study statistics the mileage of RNBs in all 52 cities with different orientations and the total quantity of solar energy received at each orientation (Supplementary material). Due to capacity limitations, Fig. 10 only includes nine representative cities. By observing Fig. 10, except for Harbin, the solar energy received by the RNB's inside is greater than that received by its outside in almost all cities. The most significant difference in solar energy absorption between the inside and outside of RNBs occurs in those with an east-west orientation. Moreover, the statistical findings from Guangzhou indicate that north-south oriented RNBs receive more solar energy than their west-east oriented counterparts under similar conditions.

4.3. PVNBs power generation potential

Installed capacity and power generation are the main criteria when assessing the potential of PV systems. Based on the approach stated in Section 3.3 and assumed both outside and inside has the same PV module specification, PVNB installed PV capacity and power generation can be evaluated using data such as the PVNB installed area, the solar radiation potential received, and PV system parameters. It should be noted that this study uses 70% of each city's RNB area as a direct input parameter to calculate the PVNB's installed PV capacity since it is

unable to account for the dynamic changes of the RNB area that is unshaded by building shadows. Figs. 11 and 12 illustrate the installed PV capacity and PVNB's power generation of the 52 cities, respectively.

Based on PV potentials of PVNB assessment results, the total installed PV capacity of the 52 cities is 2.04 GW, and the PVNB could generate 690.74 GWh of power annually. Fig. 11 and Fig. 12 show that the distribution characteristics of PVNB installed PV capacity and power generation are consistent across the 52 cities. Among the 52 cities, Shanghai has the largest potential for PVNB power generation, with a potential PVNB power generation of 107.71 GWh, more than double Suzhou's. Notably, despite not being a Tier 1 city, Shenyang's PVNB ranks fifth out of 52 cities for annual PV potential. This may be the result of the city's massive industrial and technological equipment production industries creating more noise. Additionally, cities with strong PV potential of PVNB cluster together in the Yangtze River Delta and Pearl River Delta areas, which reflects the assumption that the more developed a city is, the more complete its RNB building. The degree of RNB construction completion in each city will rise together with the level of urbanization on China's southeast coast, creating greater space for PVNB deployment and raising the potential for PVNB use in these cities.

5. Discussion

In this study, the annual power generation of PVNBs in 52 Chinese prefecture-level cities was assessed. 52 cities account for 87.7% of RNB mileages in China, with each city having more than 5 km of RNB. When a city's RNB mileage is less than 5 km, PV panels are not installed on RNBs due to scale limitations since RNBs may be spatially dispersed. Therefore, the 52 cities selected are almost representative of the PV potential of PVNBs in China.

Although this study assesses the power generation of bifacial PVNBs in

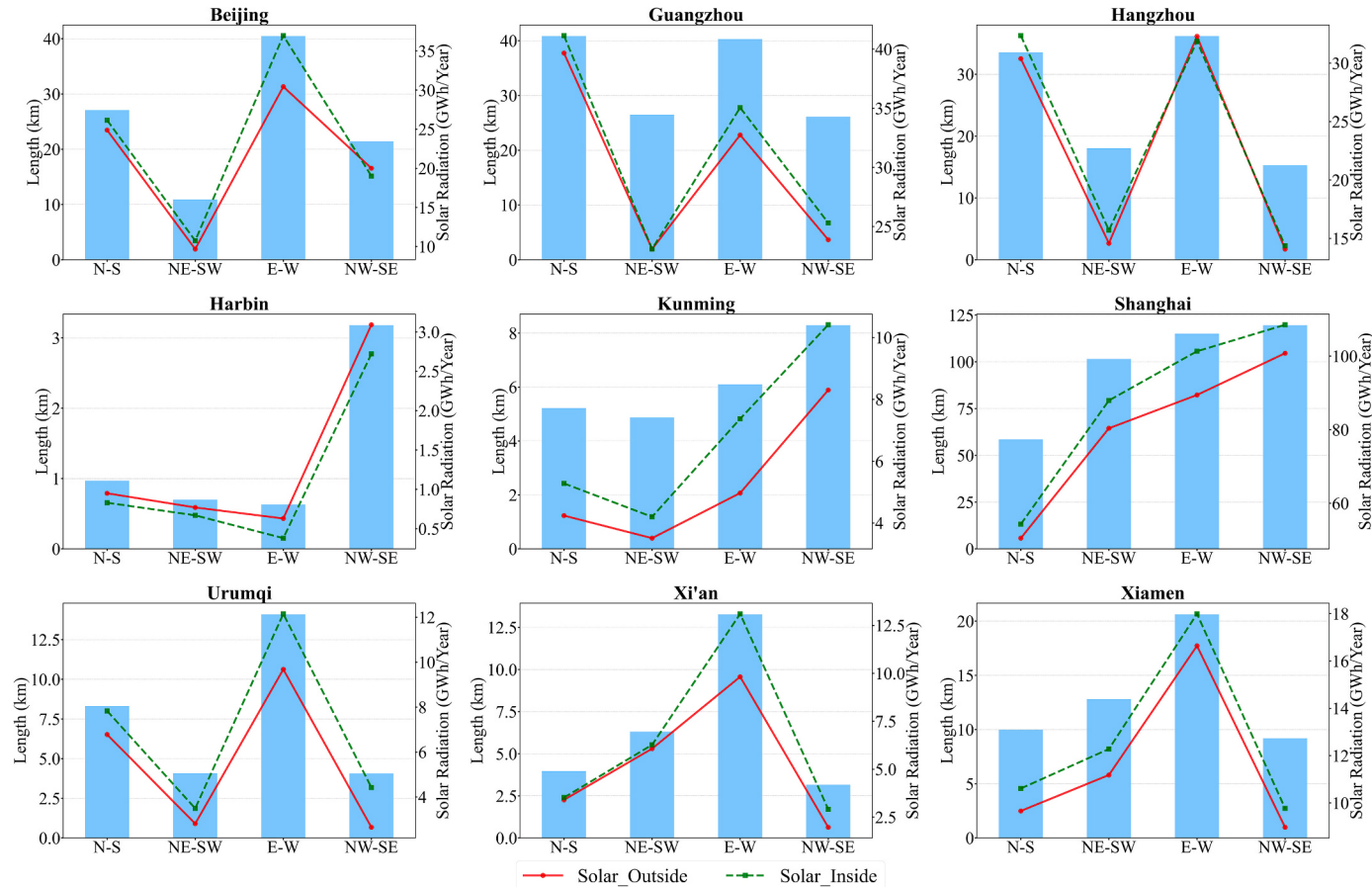


Fig. 10. Spatial distribution of the bifacial RNB's solar energy potential in 2021 for the 52 cities.

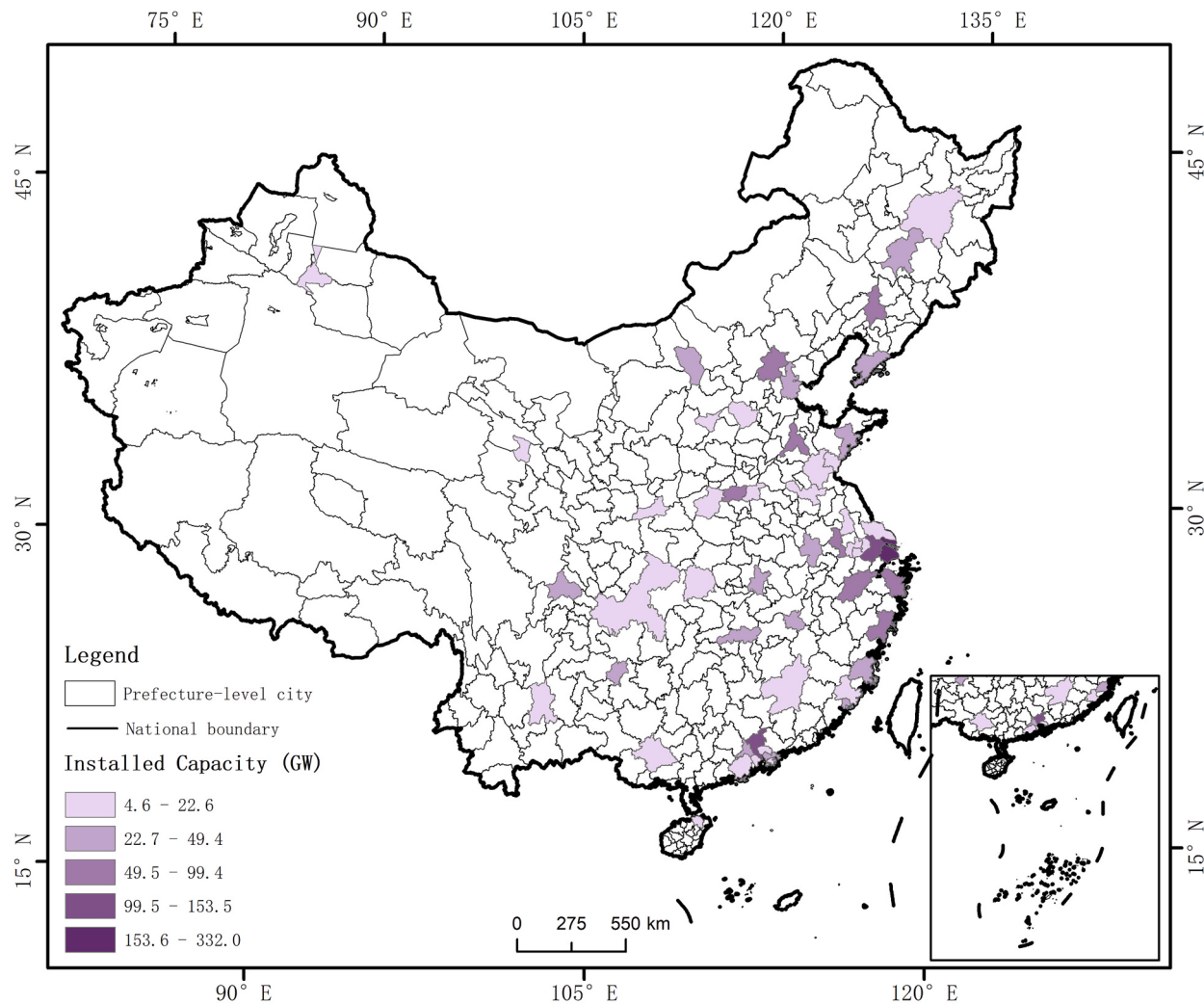


Fig. 11. Distribution characteristics of PVNB installed capacity for the 52 cities.

52 Chinese prefecture-level cities, questions about the practicality of large-scale installation and the utilization of power generated by PVNBs remain unanswered. Current PVNB projects are primarily implemented at the road scale [20]. Additionally, the study assumes the installation of two mono-facial PV panels on outside and inside of RNBs. This decision is rooted in the potential need for extensive reconstruction of all RNBs if bifacial PV panels were installed [47]. Such reconstruction would entail significant costs, possibly deviating from the initial intention of utilizing the existing RNBs. Another reason is that the efficacy of bifacial PVNBs in preventing noise pollution has not been thoroughly validated at large scales.

Assessing the economic viability of PVNBs also is a comprehensive and complex task [48]. It needs consideration of PV module cost, noise reduction advantages, PVNB's economic and ecological benefits, real-time power price, and policy support of PV. As PV conversion efficiency increases and PV module prices fall, PVNBs may be more economically feasible in the future. Additionally, integrating RNB construction with PVNB installation is more beneficial than the production of the RNB and the PV arrays separately [49]. By encouraging stakeholders to invest in the development of PVNBs, the government might reduce municipal building costs and stakeholders might acquire the electricity bill of PVNBs generated. This will ultimately promote the development of urban RNBs and improve the quality of urban habitats. In large-scale PVNB construction, the impact on the noise protection performance of RNBs and integration with the urban landscape needs to be considered. Installing PV panels on RNBs may reduce the noise

abatement effect of RNBs or have a negative effect on the local landscape or visual aesthetics [50]. Therefore, before PVNBs are used on a large scale, the noise reduction qualities of RNBs should be discussed in greater depth, and PVNB design should be integrated with urban landscape planning to enhance the landscape value of PVNBs. Additionally, building shadows have a greater influence on PVNB in high-latitude cities, as shown in Section 4.1. Therefore, a more in-depth feasibility investigation is required before installing PVNB in these cities.

The inherent intermittent and fluctuating nature of solar energy further limits the direct consumption of electricity generated by PVNBs [51]. Therefore, determining how to transmit the power generated by PVNBs to the consumer side in a stable and low-loss manner is an issue that needs to be further explored. The spatial distribution of PVNBs makes them suitable for powering nearby transportation infrastructure. Therefore, road lights, traffic signals, and other lighting facilities are potential consumers of PVNB-generated electricity. Additionally, behind-the-meter battery storage can be used to store the electricity generated by PVNBs, and this energy can then be used for electric vehicle charging stations [52] or by residents. Behind-the-meter battery storage can increase the consumption of PVNB and avoid the costs associated with integrating this energy type into the main power grid. This might be an attractive theme for further research into potential applications for PVNBs in the real world.

There are certain constraints and limitations to this study. Accurate irradiation data are the cornerstone for a precise evaluation of PV

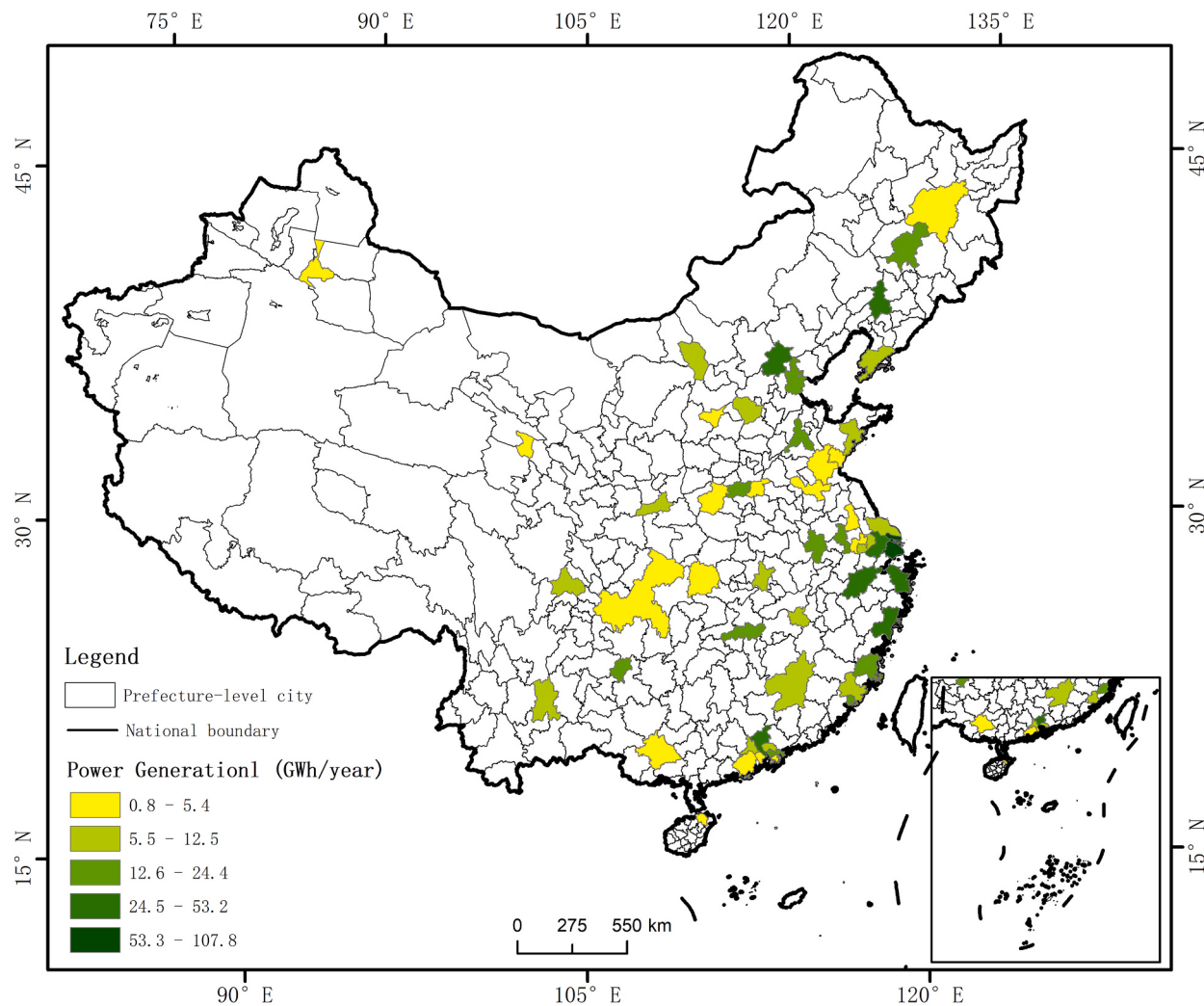


Fig. 12. Distribution characteristics of PVNB power generation in 2021 for the 52 cities.

potential. However, while the clear-sky irradiation data collected for this study has been corrected using corresponding meteorological parameters, it was interpolated to the specific point of interest using spatial input data with varying resolutions. As a result, the accuracy of the data is somewhat limited. While the emphasis of this study was on building shadows, it's essential to acknowledge that there are additional factors, like street trees, which also can have an impact on obscuring the PVNB. Besides, this study assumed that all RNBs in China are vertically installed, have only one type, and have a fixed height of 3 m. However, there are various types of RNBs in China, each type with different shapes, materials, and areas. Consequently, the area that is available for installing PV panels varies by type. These constraints and limitations need to be refined and addressed in future work.

6. Conclusion

PVNB is gaining interest as a distributed PV system. However, the assessment of PVNB's power generation needs to be refined and expanded to improve its construction and development. In this study, an accurate estimate of the PV potential of potentially exploitable PVNBs in 52 major cities in China were provided. This estimate is based on hourly radiation data and considers the impact of hourly building shadows on the solar radiation reception of PVNBs. The major results are as follows: 1) The RNB mileage in the 52 selected cities accounted for 87.7% of the total RNB mileage in China; 2) The total solar energy potential,

installed capacity, and power generation of the PVNBs in these 52 cities are 4,317 GWh, 2.04 GW, and 690.74 GWh, respectively; 3) Shadows cast by buildings can lead to a loss of approximately 30% in the power generation of PVNBs; 4) Cities with strong PV potential for PVNBs are mostly large cities in the east, while the west has very limited PV potential for PVNBs.

This study suggests that PVNBs have significant potential to supply renewable energy to cities, especially in larger cities with longer stretches of RNBs, where PVNBs can generate more power for these cities' own energy needs. In China, cities with longer mileage of RNBs are predominantly located in the east-south, which also happens to have substantial energy demands. This spatial distribution of PVNBs can boost PV power consumption, decrease PV power transfer expenses, and mitigate PV power wastage. Additionally, the results also indicate that the orientation of RNBs and building shadows significantly affects the power generation of PVNBs. Therefore, the practical implementation of PVNBs requires a more detailed economic feasibility assessment to avoid installing PV panels on RNBs that receive less solar energy. This study also demonstrates that the inner of RNBs receive as much, or even more solar energy compared to the outside of RNBs. This provides evidence of the practical value of bifacial PVNBs.

CRediT authorship contribution statement

Kai Zhang: Methodology, Investigation, Data curation, Writing -

original draft, Visualization, Writing - review & editing. **Dajiang Wang:** Software, Methodology. **Min Chen:** Writing – review & editing, Supervision, Conceptualization. **Rui Zhu:** Writing – review & editing, Conceptualization. **Fan Zhang:** Writing – review & editing, Writing – original draft, Methodology, Conceptualization. **Teng Zhong:** Writing – review & editing, Conceptualization. **Zhen Qian:** Methodology. **Yazhou Wang:** Software. **Hengyue Li:** Methodology. **Yijie Wang:** Software. **Guonian Lü:** Supervision. **Jinyue Yan:** Conceptualization.

Declaration of competing interest

The authors declare that they have no known competing financial interests or personal relationships that could have appeared to influence the work reported in this paper.

Data availability

Data will be made available on request.

Acknowledgments

This work was supported by the International Research Center of Big Data for Sustainable Development Goals (CBAS2022GSP08) and Post-graduate Research & Practice Innovation Program of Jiangsu Province (Grant No. KYCX21_1346).

Appendix A. Supplementary data

Supplementary data to this article can be found online at <https://doi.org/10.1016/j.apenergy.2024.122839>.

References

- [1] Li Z, Jiao L, Zhang B, Xu G, Liu J. Understanding the pattern and mechanism of spatial concentration of urban land use, population, and economic activities: a case study in Wuhan, China. *Geo-spat Inform Sci* 2021;24(4):678–94.
- [2] Mróczynska M, Skiba M, Bazan-Krzywoszańska A, Sztubecka M. Household standards and socio-economic aspects as a factor determining energy consumption in the city. *Appl Energy* 2020;264(5):114680.
- [3] Yuan X, Lyu Y, Wang B, Liu Q, Wu Q. China's energy transition strategy at the city level: the role of renewable energy. *J Clean Prod* 2018;205:980–6.
- [4] Zhu R, Zhang F, Yan J, Ratti C, Chen M. A sustainable solar city: from utopia to reality facilitated by GIScience. *Innov Geosci* 2023;1(1):100006.
- [5] IEA. Net Zero by 2050 A Roadmap for the Global Energy Sector. 2021, Available from: https://iea.blob.core.windows.net/assets/deebe5d-0c34-4539-9d0c-10b13d840027/NetZeroBy2050-ARoadmapfortheGlobalEnergySector_CORR.pdf. [Accessed 20, October 2022].
- [6] IEA-PVPS. Trends in PV Applications 2022. 2022, Available from: https://iea-pvps.org/wp-content/uploads/2022/09/PVPS_Trends_2022_Figures_and_Tables.pptx. [Accessed 20, October 2022].
- [7] National Energy Administration. PV construction and operation in 2021. 2022, Available from: http://www.nea.gov.cn/2022-03/09/c_1310508114.htm. [Accessed 20, October 2022].
- [8] Yan J, Yang Y, Elia Campana P, He J. City-level analysis of subsidy-free solar photovoltaic electricity price, profits and grid parity in China. *Nat Energy* 2019;4(8):709–17.
- [9] Liu S, Bi Z, Lin J, Wang X. Curtailment of renewable energy in Northwest China and market-based solutions. *Energy Policy* 2018;123(6):494–502.
- [10] China Power. Curtailment in Wind and Solar Energy is Expected to be thoroughly Solved (in Chinese). 2017, Available from: <http://www.chinapower.com.cn/guonei/20170531/7930.html>. [Accessed 20, October 2022].
- [11] Zhu R, Cheng C, Santi P, Chen M, Zhang X, Mazzarello M, et al. Optimization of photovoltaic provision in a three-dimensional city using real-time electricity demand. *Appl Energy* 2022;316:119042.
- [12] Zhang Z, Chen M, Zhong T, Zhu R, Qian Z, et al. Carbon mitigation potential afforded by rooftop photovoltaic in China. *Nat Commun* 2023;14:2347.
- [13] Zhang K, Chen M, Yang Y, Zhong T, Zhu R, Zhang F, et al. Quantifying the photovoltaic potential of highways in China. *Appl Energy* 2022;324(8):119600.
- [14] Chen Z, Jiang M, Qi L, Wei W, Yu Z, Wei W, et al. Using existing infrastructures of high-speed railways for photovoltaic electricity generation. *Resour Conserv Recycl* 2022;178(8):106091.
- [15] Hasmaden F, Zorer Gedik G, Yürek Akdag N. An approach to the design of photovoltaic noise barriers and a case study from Istanbul, Turkey. *Environ Sci Pollut Res* 2022;29(22):33609–26.
- [16] Jiang M, Qi L, Yu Z, Wu D, Si P, Li P, et al. National level assessment of using existing airport infrastructures for photovoltaic deployment. *Appl Energy* 2021; 298:117195.
- [17] Luo G, Long C, Wei X, Tang W-j. Financing risks involved in distributed PV power generation in China and analysis of countermeasures. *Renew Sust Energ Rev* 2016; 63:93–101.
- [18] Clavadetscher L, Nordmann T, editors. 100 kW Gridconnected PV plant A13 in Switzerland-10 years and 1'000'000 kWh Later. Routledge; 2020.
- [19] Gu M, Liu Y, Yang J, Peng L, Zhao C, Yang Z, et al. Estimation of environmental effect of PVNB installed along a metro line in China. *Renew Energy* 2012;45: 237–44.
- [20] Energy HR. Photovoltaic Noise Barriers. Washington, DC, USA: Office of Natural Environment; 2017.
- [21] Nordmann CL. PV on noise barriers. *Prog Photovolt Res Appl* 2004;12(6):485–95.
- [22] Qian Z, Chen M, Yang Y, Zhong T, Zhang F, Zhu R, et al. Vectorized dataset of roadside noise barriers in China using street view imagery. *Earth Syst Sci Data* 2022;14(9):4057–76.
- [23] Li M, Virguez E, Shan R, Tian J, Gao S, Patiño-Echeverri D. High-resolution data shows China's wind and solar energy resources are enough to support a 2050 decarbonized electricity system. *Appl Energy* 2022;306:117996.
- [24] Li J, Huang J. The expansion of China's solar energy: challenges and policy options. *Renew Sust Energ Rev* 2020;132:110002.
- [25] Zhang K, Qian Z, Yang Y, Chen M, Zhong T, Zhu R, et al. Using street view images to identify road noise barriers with ensemble classification model and geospatial analysis. *Sustain Cities Soc* 2022;78(4):103598.
- [26] Kanellis M, de Jong MM, Slooff L, Debije MG. The solar noise barrier project: 1. Effect of incident light orientation on the performance of a large-scale luminescent solar concentrator noise barrier. *Renew Energy* 2017;103:647–52.
- [27] Debije MG, Tzikas C, de Jong MM, Kanellis M, Slooff LH. The solar noise barrier project: 3. The effects of seasonal spectral variation, cloud cover and heat distribution on the performance of full-scale luminescent solar concentrator panels. *Renew Energy* 2018;116:335–43.
- [28] Faturrochman GJ, de Jong MM, Santbergen R, Folkerts W, Zeman M, Smets AHM. Maximizing annual yield of bifacial photovoltaic noise barriers. *Sol Energy* 2018; 162(17–18):300–5.
- [29] Vallati A, Vollaro RDL, Tallini A, Cedola L. Photovoltaics noise barrier: acoustic and energetic study[J]. *Energy Procedia* 2015;82:716–23.
- [30] Zhong T, Zhang K, Chen M, Wang Y, Zhu R, Zhang Z, et al. Assessment of solar photovoltaic potentials on urban noise barriers using street-view imagery. *Renew Energy* 2021;168:181–94.
- [31] Wang Y. Application of solar noise barrier power generation system envisaged on urban elevated roads. *J Phys Conf Ser* 2020;1549(5):52118.
- [32] Wadhawan SR, Pearce JM. Power and energy potential of mass-scale photovoltaic noise barrier deployment: a case study for the U.S. *Renew Sust Energ Rev* 2017;80: 125–32.
- [33] He Q, Song Y, Liu Y, Yin C. Diffusion or coalescence? Urban growth pattern and change in 363 Chinese cities from 1995 to 2015. *Sustain Cities Soc* 2017;35(3): 729–39.
- [34] Yu Q, Li G. Pybdshadow. <https://github.com/n1o1/pybdshadow>; 2022.
- [35] Wikipedia. Sunrise equation. 2022, Available from: https://en.wikipedia.org/wiki/Sunrise_equation. [Accessed October 12, 2022].
- [36] Demain C, Journée M, Bertrand C. Evaluation of different models to estimate the global solar radiation on inclined surfaces. *Renew Energy* 2013;50:710–21.
- [37] Raptis PI, Kazadzis S, Psiloglou B, Kouremeti N, Kosmopoulos P, Kazantzidis A. Measurements and model simulations of solar radiation at tilted planes, towards the maximization of energy capture. *Energy* 2017;130:570–80.
- [38] Reindl DT, Beckman WA, Duffie JA. Evaluation of hourly tilted surface radiation models. *Sol Energy* 1990;45(1):9–17.
- [39] Badescu V. Modeling solar radiation at the Earth's surface: recent advances. Berlin: Springer; 2008.
- [40] Duffie JA, Beckman WA. In: Duffie John A, Beckman William A, editors. *Solar engineering of thermal processes*. 4th ed. Hoboken: John Wiley; 2013.
- [41] Liu BYH, Jordan RC. The long-term average performance of flat-plate solar-energy collectors: with design data for the US, its outlying possessions and Canada. *Sol Energy* 1963;7(2):53–74.
- [42] Kim K, Byon J, Kim H. Heat Island intensity in Seongseo, Daegu, South Korea - a rural suburb containing large areas of water. *J Environ Sci Int* 2013;22(10): 1337–44.
- [43] Huang S, Rich PM, Crabtree RL, Potter CS, Fu P. Modeling monthly near-surface air temperature from solar radiation and lapse rate: application over complex terrain in Yellowstone National Park. *Phys Geogr* 2008;29(2):158–78.
- [44] Suri M, Hofierka J. A new GIS-based solar radiation model and its application to photovoltaic assessments. *Trans GIS* 2004;8(2):175–90.
- [45] Qi L, Jiang M, Lv Y, Yan J. A celestial motion-based solar photovoltaics installed on a cooling tower. *Energy Convers Manag* 2020;216(8):112957.
- [46] Berwäl AK, Kumar S, Kumari N, Kumar V, Haleem A. Design and analysis of rooftop grid tied 50 kW capacity solar photovoltaic (SPV) power plant. *Renew Sust Energ Rev* 2017;77:1288–99.
- [47] Gu W, Ma T, Ahmed S, Zhang Y, Peng J. A comprehensive review and outlook of bifacial photovoltaic (bPV) technology. *Energy Convers Manag* 2020;223:113283.
- [48] Cavallaro F, Nocera S. Are transport policies and economic appraisal aligned in evaluating road externalities? *Transp Res Part D: Transp Environ* 2022;106: 103266.
- [49] De Schepper E, Van Passel S, Manca J, Thewys T. Combining photovoltaics and sound barriers—A feasibility study. *Renew energy* 2012;46:297–303.

- [50] ANAS. State-of-the-art on secondary functions for pavements and noise screens. 2014, Available from: https://www.cedr.eu/download/other_public_files/research_programme/call_2012/road_noise/distance/DISTANCE-BRRC-D31-V01-010415-State-of-the-art-on-secondary-functions-of-noise-barriers-and-pavements.pdf. [Accessed 20, October 2022].
- [51] Kuang Y, Zhang Y, Zhou B, Li C, Cao Y, Li L, et al. A review of renewable energy utilization in islands. *Renew Sust Energ Rev* 2016;59(2):504–13.
- [52] Zhang K, Chen M, Zhu R, Zhang F, Zhong T, Lin J, et al. Integrating photovoltaic noise barriers and electric vehicle charging stations for sustainable city transportation. *Sustain Cities Soc* 2023;100:104996.